Tandem catalysis enables chlorine-containing waste as chlorination reagents

Mingyang Liu , Xinbang Wu & Paul J. Dyson ✉

Chlorinated compounds are ubiquitous. However, accumulation of chlorine-containing waste has a negative impact on human health and the environment due to the inapplicability of common disposal methods, such as landfill and incineration. Here we report a sustainable approach to valorize chlorine-containing hydrocarbon waste, including solids (chlorinated polymers) and liquids (chlorinated solvents), based on copper and palladium catalysts with a $NaNO_3$ promoter. In the process, waste is oxidized to release the chlorine in the presence of N-directing arenes to afford valuable aryl chlorides, such as the FDA-approved drug vismodegib. The remaining hydrocarbon component is mineralized to afford CO, CO_2 and H_2O. Moreover, the CO and CO_2 generated could be further utilized directly. Thus, chlorine-containing hydrocarbon waste, including mixed waste, can serve as chlorination reagents that neither generate hazardous by-products nor involve specialty chlorination reagents. This tandem catalytic approach represents a promising method for the viable management of a wide and diverse range of chlorine-containing hydrocarbon wastes.

Chlorinated compounds are ubiquitous in industrialized societies, as the physical and chemical properties of hydrocarbons are extensively modified (and improved) following chlorination. Thus, chlorine-containing hydrocarbons are widely used as plastics[1,2], rubbers[3–5], resins[6,7] and solvents[8–10], and have applications as intermediates used in the synthesis of agrochemicals and pharmaceuticals[11,12], or are even present in agrochemical and pharmaceutical products[13–16]. Despite their enormous utility, chlorine-containing hydrocarbons are persistent in the environment or decompose to release toxic compounds, which can accumulate in the food chain. Exposure to chlorinated waste is even associated with suppression of the immune system and cancer, and yet methods to dispose of waste chlorine-containing hydrocarbons are currently inadequate[17–19].

Chlorine-containing hydrocarbon waste is one of the most problematic types of waste because of the large scale of such waste and the common industrial approaches used to deal with it (landfill and incineration), which lead to the formation of hazardous products, including dioxins and corrosive gases such as HCl and Cl_2. Safe disposal of chlorinated waste is therefore highly challenging (Fig. 1), with both pyrolysis and hydrocracking being unsuitable, as they result in the same problems as industrial incineration[20–24].

Although catalytic hydrocracking has been extensively investigated for upgrading a range of polymers, when applied to chlorinated polymers, deactivation of the catalyst is usually observed[25–28]. Hence, a two-step process consisting of dechlorination followed by decomposition has been reported, but this is expensive and largely unviable[20,29–33]. Recent approaches used for the destruction of polyvinyl chloride (PVC) are summarized in Supplementary Table 1 (note that HCl is produced in the majority of cases and is typically neutralized in a second step). Recently an electrochemical dechlorination method was reported for PVC, but only partial dechlorination (<20% conversion of Cl groups) was achieved and the method might be difficult to upscale[34]. Likewise, waste chlorinated solvents are problematic, with incineration being the conventional method used to dispose of them, as bioremediation is slow[35,36]. Electrochemical dechlorination of chlorinated hydrocarbon compounds has been reported, but suffers from low reaction rates and low Faradaic efficiencies (typically <50%)[37,38]. On account of these limitations for the reported treatments (which require corrosive reagents or lead to corrosive HCl emissions), there does not appear to be a sustainable, scalable method that efficiently eliminates different types of chlorinated hydrocarbon waste.
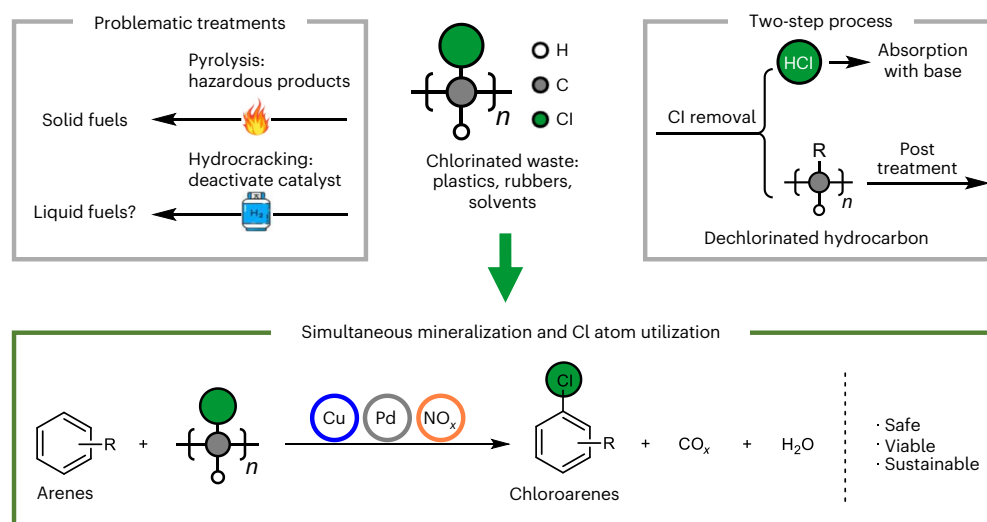
Institute of Chemical Sciences and Engineering, Ecole Polytechnique Fédérale de Lausanne (EPFL), Lausanne, Switzerland. ✉e-mail: paul.dyson@epfl.ch

Fig. 1 | Methods development. Methods developed for the possible elimination of chlorinated wastes and the approach described in this work in which various chlorinated wastes are employed as chlorination reagents for the synthesis of fine chemicals, with concomitant mineralization of the hydrocarbon component.

Extending on the achievements in Pd-catalysed C−H bond chlorination[39–42] and Cu/NO$_x$-catalysed C−C bond oxygenation[43–46], we integrated the two reactions to afford a safe, sustainable and economically viable strategy to use chlorinated waste as chlorination reagents (Fig. 1). The approach simultaneously generates CO/CO$_2$, via Cu/NO$_x$-catalysed oxygenation of the hydrocarbon component, and chloride, which is transferred via Pd-catalysed C−H bond chlorination, to afford valuable aryl chlorides.

Results and discussion
Initial investigation of the reaction conditions
The high polarity of C−Cl bonds compared to C−H bonds in chlorine-containing hydrocarbon waste facilitates interactions with catalysts and can lead to their activation and functionalization[47,48]. Following C−Cl bond activation, transfer of the chlorine to a substrate, and mineralization of the hydrocarbon component of the waste, must be initiated. Commencing with conditions similar to those reported for the transfer of chlorine atoms in chlorophenol pollutants to arenes[49], a Cu-catalysed aerobic reaction employing 7,8-benzoquinoline **1a** as substrate and PVC (molecular weight, M_w: 100,000) as chlorination reagent, led to only trace quantities of the anticipated chlorinated product, namely, 10-chlorobenzoquinoline **1b** (Supplementary Fig. 1). Since Pd catalysts are widely used to form C–X bonds[42], bimetallic systems consisting of Cu and Pd catalysts were evaluated and found to generate the chlorinated product **1b** (Fig. 2a, entries 1–5). The combination of homogeneous Cu(NO$_3$)$_2$ and heterogenous Pd catalysts (PdO, Pd/C, Pd(OH)$_2$/C) remarkably enhances the yield of **1b** to 83–85% (Fig. 2a, entries 1–3). Notably, the homogeneous Pd complexes are less efficient catalysts than heterogenous Pd catalysts (Fig. 2a, entries 4 and 5), which may be attributed to the strong coordination of the N-directing substrate leading to stable complexes that are less active[50,51]. Optimization of the NaNO$_3$ concentration afforded the chlorinated product **1b** in 99% yield (Fig. 2a, entry 7). The heterogenous PdO may be recovered by filtration and reused without loss in activity (Supplementary Fig. 11). Further details concerning the optimization of the reaction parameters are provided in Supplementary Figs. 1–10.

The gaseous products from the reaction were analysed by gas chromatography (GC) with CO and CO$_2$ obtained in 15 and 81% yield, respectively, based on the carbon content of PVC (Fig. 2b), confirming that the hydrocarbon component of PVC is mineralized in near-quantitative yield (the formation of water was detected by ^{1}H NMR spectroscopy;

see below). Note that these gases were not observed in a control experiment without PVC. Notably, in the absence of PdO catalyst (Supplementary Table 2, entry 20), CO is obtained in 83% yield (with **1b** formed in 12% yield), suggesting that PdO promotes the oxidation of CO to CO$_2$ (ref. 52). Consequently, it was found that in the presence of PdO, that is, under the standard reaction conditions, the selectivity to CO can be improved to 48% by adding bis(benzene)chromium (Fig. 2b and Supplementary Table 2), with the chlorinated product **1b** formed in 72% yield. The product distribution (using PVC and **1a** as substrates) was quantified, and confirms that the PVC was completely mineralized into gases (CO and CO$_2$) and the Cl atoms converted into **1b** and excess HCl (Supplementary Fig. 12). Moreover, the unpurified gas stream was directly used in the carbonylation of 1-phenylethane-2,3-diol[53] (consuming the CO generated) and in the cycloaddition of CO$_2$ to styrene oxide (fixing the CO$_2$ produced) affording styrene carbonate, thereby valorizing all the carbon atoms in PVC (Supplementary Fig. 13).

The depolymerization of PVC was monitored by gel permeation chromatography (GPC) and chromatograms before and after reaction (Fig. 2c) show that the characteristic peaks of PVC (with different molecular weights) completely disappear. Only signals corresponding to small molecules, that is, **1a** and **1b**, remain, confirming the total depolymerization of the polymers. ^{1}H NMR spectroscopy shows that after the reaction (Fig. 2d; see caption for details of the reaction conditions), the characteristic peaks attributed to the 10-H of substrate **1a** and the α/β-Hs of PVC are no longer present, and only signals attributable to the chlorinated product **1b** and H$_2$O are observed (for comparison, the ^{1}H NMR spectrum of **1b** is provided in Supplementary Fig. 14). The region between 1 and 5 ppm is clear, which is where signals derived from alkyl monomers or oligomers would be expected to be observed. Thus, **1b** and water are the only liquid products obtained during the reaction.

Scope of the chlorinated waste
Solid waste derived from commercial chlorinated plastics and rubbers is typically manufactured with other components present, including plasticizers, fillers and pigments, to provide rigidity, elasticity, colour and other properties[34]. To explore the utility of our method when applied to real waste, a range of postconsumer products were evaluated (Table 1). Using a PVC-based water pipe, electrical conduit and electric wire (**P1**; Supplementary Fig. 15), chlorinated product **1b** was obtained in yields of 80 to 99%. Transparent polyvinylidene chloride (PVDC, **P2**) is extensively used as a packaging material for food
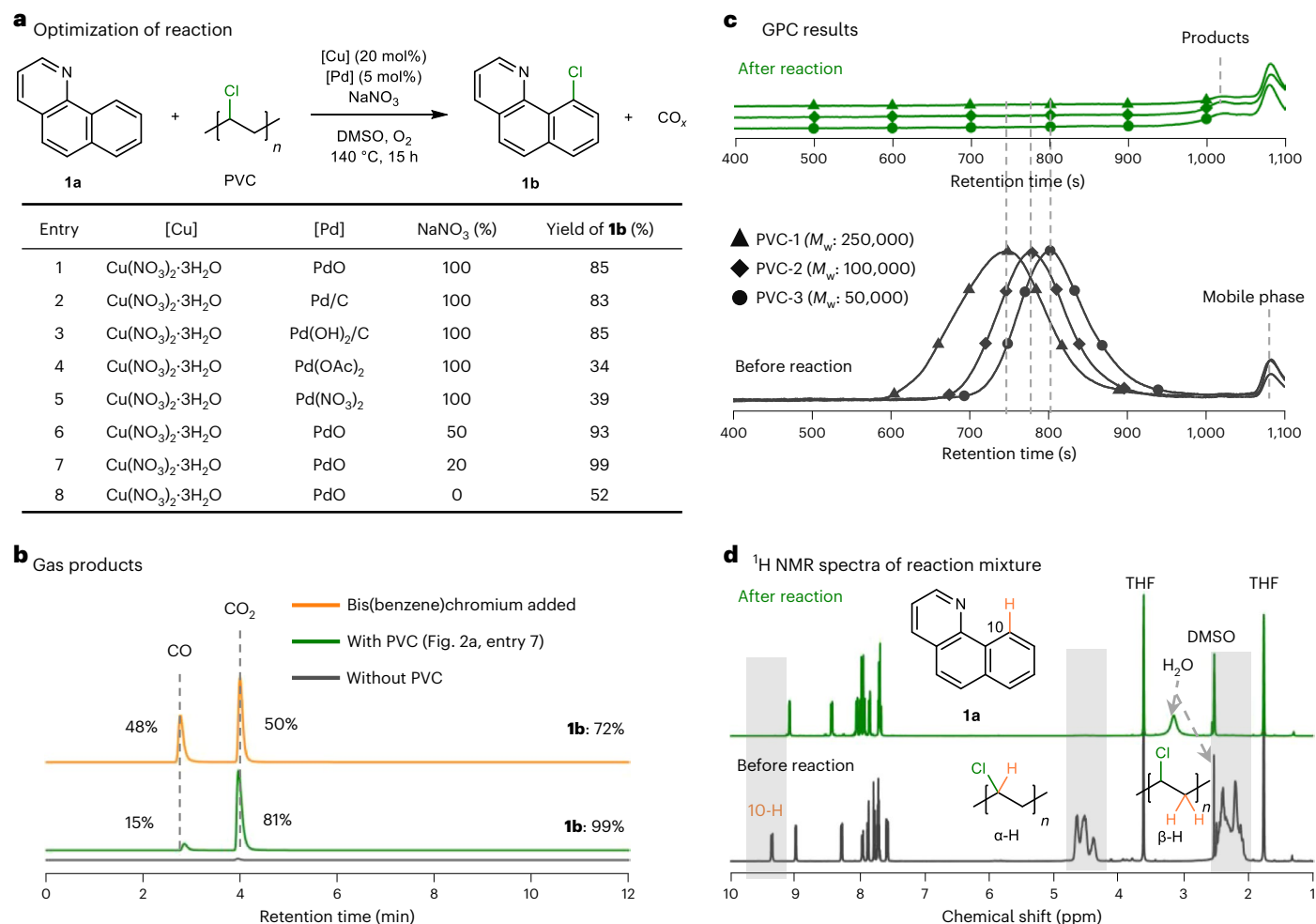
a Optimization of reaction

Entry	[Cu]	[Pd]	NaNO$_3$ (%)	Yield of **1b** (%)
1	Cu(NO$_3$)$_2$·3H$_2$O	PdO	100	85
2	Cu(NO$_3$)$_2$·3H$_2$O	Pd/C	100	83
3	Cu(NO$_3$)$_2$·3H$_2$O	Pd(OH)$_2$/C	100	85
4	Cu(NO$_3$)$_2$·3H$_2$O	Pd(OAc)$_2$	100	34
5	Cu(NO$_3$)$_2$·3H$_2$O	Pd(NO$_3$)$_2$	100	39
6	Cu(NO$_3$)$_2$·3H$_2$O	PdO	50	93
7	Cu(NO$_3$)$_2$·3H$_2$O	PdO	20	99
8	Cu(NO$_3$)$_2$·3H$_2$O	PdO	0	52

b Gas products

c GPC results

d ^{1}H NMR spectra of reaction mixture

Fig. 2 | Reaction optimization and characterization of the products.
a, Optimization of the reaction parameters. Reaction conditions:
7,8-benzoquinoline **1a** (0.25 mmol), PVC (1.5 equiv., 0.375 mmol), Cu catalyst
(20 mol%, 0.05 mmol), Pd catalyst (5 mol%, 0.0125 mmol), NaNO$_3$ (0–100 mol%),
biphenyl (0.2 mmol, internal standard), dimethylsulfoxide (DMSO; 2 ml), O$_2$
(3 bar), 140 °C, 15 h. Yield of gas and liquid products was determined by GC. **b**, GC
of gas-phase products after reaction (reaction conditions correspond to those

in **a**, entry 7) and the control experiment without PVC. **c**, GPC chromatograms
before and after reaction. **d**, ^{1}H NMR spectra of reaction mixture before and after
reaction (reaction conditions correspond to those in **a**, entry 7). THF-d$_8$ was
used instead of DMSO-d$_6$ to dissolve the reaction mixture before reaction, as
PVC is insoluble in DMSO. THF-d$_8$ was also added into the reaction mixture after
reaction, for the ^{1}H NMR spectroscopic analysis.

and pharmaceutical products, and in the forms of raw powder and
blister affords **1b** in 99% yield. Polyepichlorohydrin (PECH, **P3**) with
primary Cl groups was also tested and gave **1b** in 99% yield. Rubber has
short polymeric chains and extensive cross-linkages, endowing it with
greater elasticity than most plastics, but making it more challenging to
depolymerize[54,55]. Nonetheless, neoprene rubber (**P4**), raw chunks and
vacuum tube, both afford **1b** in a similar yield, that is, 80–82%, showing
that the cross-linkages are transformed under the reaction conditions.
Substrate **1a** was also chlorinated in the presence of copolymers with
hetero-oxygen atoms, that is, poly(epichlorohydrin-co-ethylene oxide)
(PECHEO, **P5**) and poly(epichlorohydrin-co-CO$_2$) (PECHC, **P6**), with **1b**
obtained in 99% yield. We simulated real waste streams by employing a
mixture of several types of PVC-based and polyolefin (polyethylene (PE)
and polypropylene (PP)) plastic waste in the chlorination of **1a** under
the standard reaction conditions. The polyolefins remain intact after
reaction, whereas the PVC was consumed to afford chlorinated product
1b in 87% yield. The use of mixed plastics demonstrates the possibility
to selectively valorize PVC from mixtures containing polyolefins and
potentially other types of plastic waste, although it is likely that real
waste streams would require washing before use, as is common in other
plastic upcycling processes[56,57].

In addition to plastic waste, various liquid chlorine-containing
hydrocarbon wastes were evaluated as chlorination reagents (Table 1).
Chlorinated solvents and reagents are extensively used in chemistry
and for cleaning purposes in many industries[8,9,58]. For example, dichlo-
romethane (DCM) is the most extensively used solvent by volume in the
pharmaceutical industry (~18%), and requires safe disposal to minimize
damage to human health (it is a carcinogen) and damage to the environ-
ment. DCM and other commonly used chlorinated solvents (**C1** and
C4–**C8**) are good chlorination reagents in our system (40–87%), with
the exception of chloroform (**C2**) and tetrachloromethane (**C3**). Note
that perchloroethene (**C8**) is the most widely used solvent in dry clean-
ing[58]. Other mono- and dichlorinated alkanes (**C9** and **10**), alkenes (**C11**)
and alkylbenzenes (**C13** and **14**) serve as excellent sources of chlorine,
to afford chlorinated product **1b** in 91–99% yield. Chlorocyclohexane
(**C12**) is a poor chlorination reagent, whereas epichlorohydrin (**C15**)
and epichlorohydrin carbonate (**C16**) perform chlorination well, with
both affording **1b** in 98% yield.

Actual laboratory waste was used in the reaction, obtained from
the synthesis of the ionic liquid 1-butyl-3-methylimidazolium chloride
([BMIM]Cl) prepared from the reaction of excess butyl chloride in DCM
(Table 1). Following isolation of the [BMIM]Cl product, the chlorinated

Table 1 | Application of chlorinated polymers, including postconsumer waste and liquid waste, in the chlorination reaction of 1a to 1b
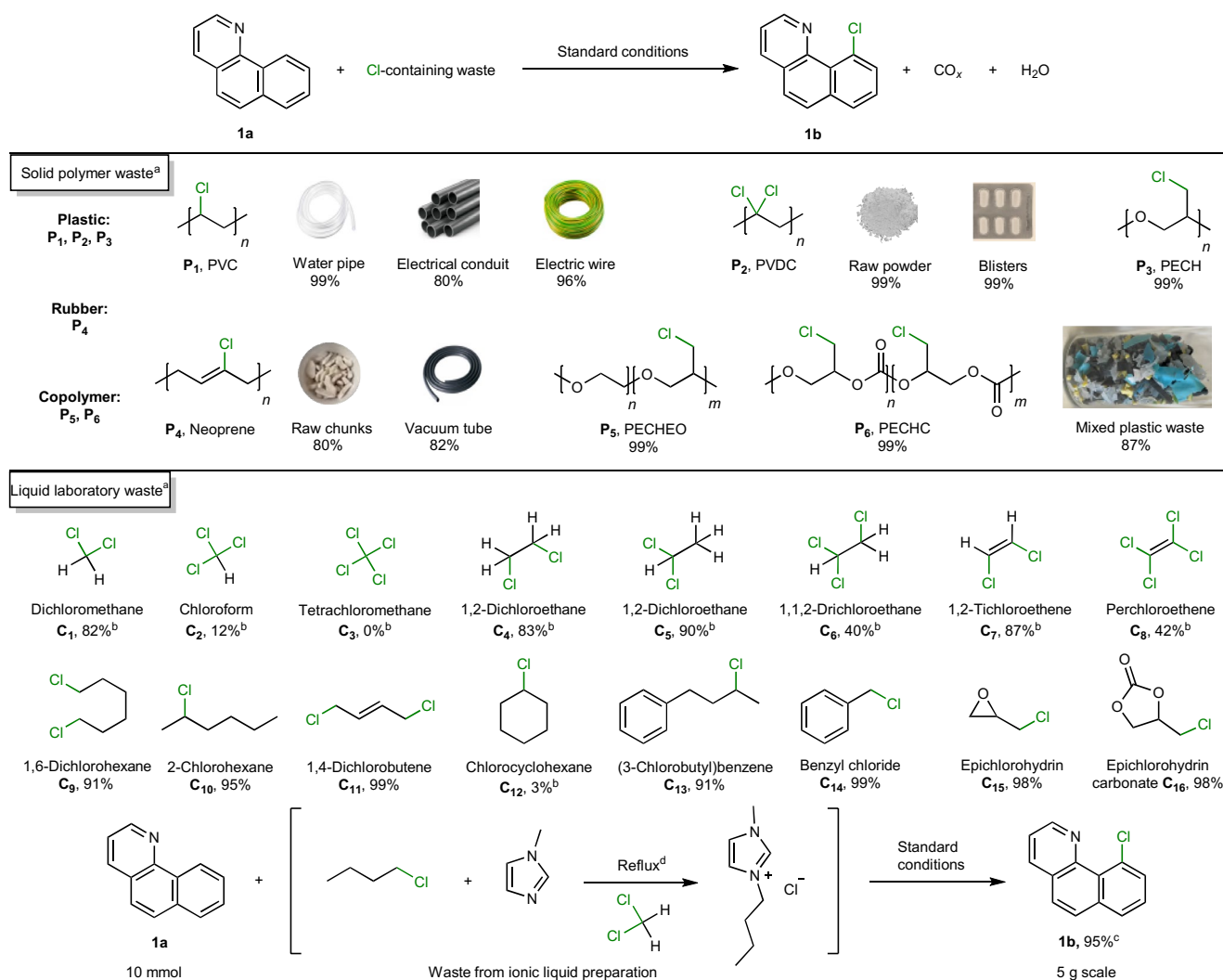
Reaction conditions: [a]7,8-benzoquinoline **1a** (0.25 mmol), chlorinated waste (1.5 equiv., 0.375 mmol, calculated on the basis of the content of chlorine—the chlorine content of postconsumer waste was determined by Schöniger combustion), Cu(NO₃)₂·3H₂O (20 mol%, 0.05 mmol), PdO (5 mol%, 0.0125 mmol), NaNO₃ (20 mol%, 0.05 mmol), biphenyl (0.2 mmol, internal standard), DMSO (2 ml), O₂ (3 bar), 140 °C, 15 h. [b]Chlorinated waste (3 equiv., 0.75 mmol). [c]7,8-Benzoquinoline **1a** (30 mmol), 5.4 gram scale, compressed air (8 bar), 20 h. [d]1-Methylimidazole (20 mmol), 1-chlorobutane (30 mmol) and dichloromethane (20 ml), reflux at 60 °C, 48 h. The mixed waste contained by mass: 25% PVC water pipe, 25% PVC electrical conduit, 25% PVC electric wire and 25% polyolefin plastic waste (PE and PP). Yield of the chlorinated product **1b** was determined by GC.

Substrate scope of arenes

Chlorinated arenes are widely employed as pharmaceuticals, agrochemicals, dyes and solvents[13,42,60]. Chlorination of arenes typically involves toxic and corrosive reagents (sulfuryl dichloride, HCl, Cl₂)[61,62] or the application of expensive reagents, such as chloramines, which have a low atom economy[42,63,64]. In contrast, using chlorinated waste as chlorination reagents may be considered as an inexpensive, benign

and sustainable method that alleviates problems related to the disposal of such waste. To investigate the scope of this method, a range of aromatic and heteroaromatic substrates with N-directing groups were evaluated using colourless PVC water pipe as the chlorination reagent (Table 2). Pyridine-directing arenes with various electron-withdrawing and electron-donating groups were chlorinated with high selectivity to afford regioselective aryl *ortho*-dichloride products (**2b**–**7b**) or aryl *ortho*-monochloride products (**8b**, **9b**) in 74–98% yield. The impact of functional groups on the pyridine-directing group (**10a**, **11a**) is critical to control the selectivity of *ortho*-di- or monochloride products (**10b**, **11b**). Product **12b** is an intermediate in the synthesis of vismodegib, a drug used for the treatment of basal cell carcinoma (see 'Application to pharmaceutical synthesis' below)[65,66]. Pyrimidine-directing arenes (**13a**–**18a**) also afford the expected chlorinated products, but in slightly lower selectivity of *ortho*-di- or monochloride products. Interestingly, arenes with pyrazol-directing groups (**19a**–**24a**) were selectively monochlorinated in good yield (72–81%). Arenes with 8-aminoquinoline (bidentate,

Table 2 | Evaluation of the substrate scope
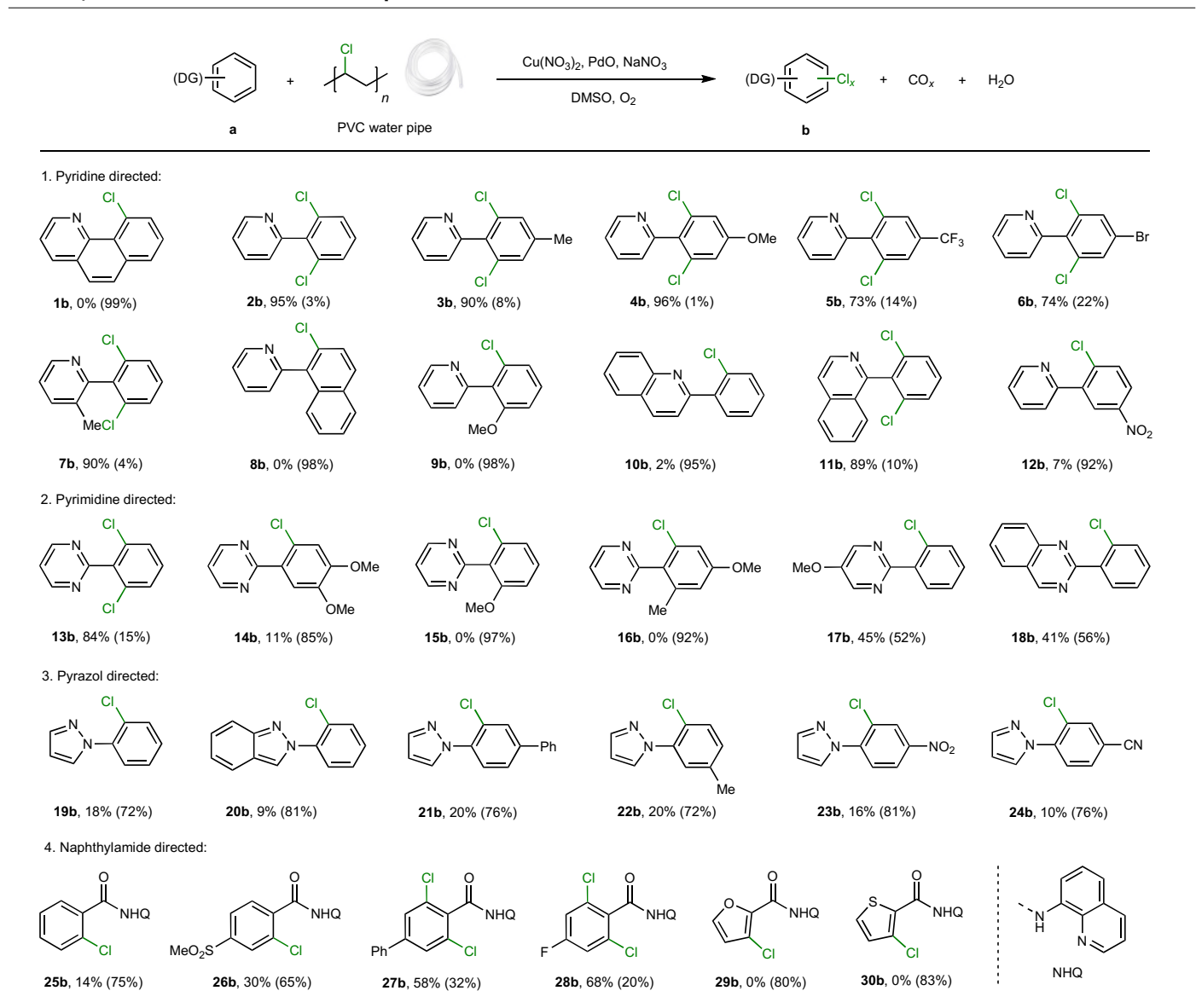
Reaction conditions: arene **a** (0.25 mmol), PVC water pipe (1.5 equiv., 0.375 mmol), Cu(NO$_3$)$_2$·3H$_2$O (20 mol%, 0.05 mmol), PdO (5 mol%, 0.0125 mmol), NaNO$_3$ (20 mol%, 0.05 mmol), biphenyl (0.2 mmol), DMSO (2 ml), O$_2$ (3 bar), 140 °C, 15 h. Yields of *ortho*-dichloride products are reported and yields of monochloride products are included in the brackets.

NHQ)-directing groups (**25a**–**30a**) were also mono- or dichlorinated, but in slightly lower yields (58–80%). Compounds **25b**–**27b** are important synthetic intermediates of active EP$_1$ antagonists[67] and positive allosteric modulators[68]. In general, the excess PVC employed in the reaction is to ensure high product yields and does not affect the selectivity for *ortho*-di- or monochloride products. Employing PVC loadings containing stochiometric amounts of chlorine in the reaction slightly decrease the product yield. For example, when employing **12a** as substrate (Supplementary Fig. 17), decreasing the PVC loading from 1.5 to 0.75 equiv. decreases the yield of monochloride product from 92% (Cl atom economy 71%) to 65% (Cl atom economy 97%).

Application to pharmaceutical synthesis

This method using Cl-containing waste as a chlorination reagent was applied to the synthesis of the FDA-approved anticancer drug vismodegib (Fig. 3). On the basis of a retrosynthetic analysis of vismodegib, the pyridine-directed arene **12a** and NHQ-directed arene **26a** were selected as the starting materials[66]. *Ortho*-C–H chlorination of **12a** followed by reduction gives 4-chloro-3-pyridin-2-ylaniline, **31b**. Compound

26a was chlorinated using the standard conditions (see caption to Fig. 3) and hydrolysed to afford 2-chloro-4-(methylsulfonyl)benzoic acid, **32b**. Condensation of **31b** and **32b** affords vismodegib, with an overall yield of 68%. The two Cl groups in vismodegib are derived from the waste PVC water pipe, and the spectroscopic and analytical data (Supplementary Figs. 18–20 and Supplementary Table 4) indicate that the route should be compatible with the stringent purity requirements of the pharmaceutical industry. Green metrics calculations of the process mass intensity (PMI) and environmental factor (E-factor) were performed (Fig. 3), demonstrating that the chlorination method has a similar efficiency and sustainability to a reported C–H chlorination method[63].

Mechanistic studies

The reaction mechanism of this reliable and robust chlorination method was probed with a view to establishing the role of the Cu(NO$_3$)$_2$ and PdO catalysts, the NaNO$_3$ promoter and the strong solvent effect of dimethylsulfoxide (DMSO). The reaction may be divided into three parts: (1) dechlorination of chlorinated waste; (2) depolymerization/
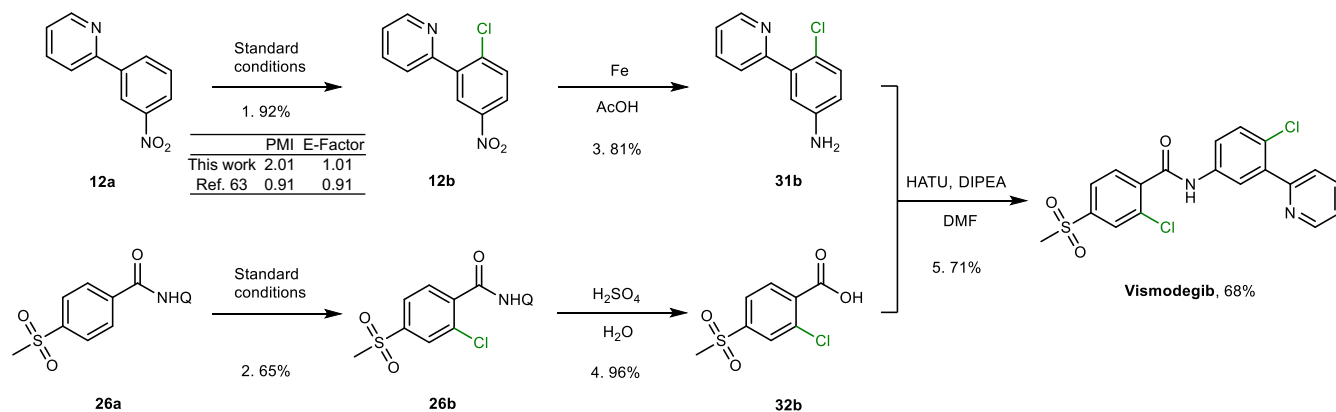
Fig. 3 | Synthesis of vismodegib. Reaction conditions: steps 1 and 2 were performed using the standard conditions, that is, **12a** or **26a** (0.25 mmol), PVC water pipe (1.5 equiv., 0.375 mmol), $Cu(NO_3)_2 \cdot 3H_2O$ (20 mol%, 0.05 mmol), PdO (5 mol%, 0.0125 mmol), $NaNO_3$ (20 mol%, 0.05 mmol), DMSO (2 ml), O_2 (3 bar), 140 °C, 15 h; step 3, **12b** (0.50 mmol), Fe powder (5.0 mmol) and AcOH (4 ml), 80 °C, 0.5 h; step 4, **26b** (0.45 mmol) and 40% H_2SO_4 aqueous solution (2 ml), 120 °C, 12 h; step 5, **31b** (0.20 mmol), **32b** (0.20 mmol), 1-[bis(dimethylamino)

methylene]-1H-1,2,3-triazolo[4,5-b]pyridinium 3-oxide hexafluorophosphate (HATU; 0.12 mmol), N,N-diisopropylethylamine (DIPEA; 0.21 mmol) and anhydrous DMF (2 ml), room temperature, 24 h. GC yields of each step and overall yield of vismodegib are based on **12a**. Green metrics including PMI and E-factor of step 1 are included. See Supplementary Information for details of the calculations.

decomposition of the dechlorinated waste; and (3) chlorination of the arene substrate. Initially, several potential, model chlorination reagents were tested under the standard reaction conditions (Extended Data Fig. 1). Reagents without an α-H and β-H (**1c**), or chloride salts without H^+ (**6c**, **7c**), were inactive or sparingly active (0–8%). Reagents with either an α-H (**2c**) or β-H (**3c**) only afforded the chlorinated product **1b** in modest yield (46% and 39%, respectively). In contrast, reagents containing both α- and β-H (**4c**, **5c**) provide **1b** in good yield (78–90%), which demonstrates that removable α- and β-H are required for chlorination. The application of acetic acid (provides excess H) and NaCl (**6c**, condition 2) or alternatively HCl (**8c**) as chlorination reagents notably improves the yield of **1b**, further confirming the importance of H (cleavable C–H bonds or H^+). These control experiments suggest that in the initial dechlorination step HCl is generated, which acts as the chlorination reagent, and the pH of the reaction mixture confirms the formation of HCl (Supplementary Fig. 21).

Next, the dechlorination of the model reagent 1-phenylethyl chloride (**4c**) was studied (Extended Data Fig. 2). Using CuO (Extended Data Fig. 2, entry 1) or $NaNO_3$ (Extended Data Fig. 2, entry 2) as the catalyst in DMSO, benzoic acid is the dominant product, revealing simultaneous dechlorination and carbon–carbon bond cleavage. With PdO (Extended Data Fig. 2, entry 3) or without catalyst (Extended Data Fig. 2, entry 4), styrene (obtained by dehydrochlorination) is the main product with 1-phenylethanol (obtained by dechlorohydroxylation) obtained in lower quantities. Dechlorination is not observed in the absence of O_2 (Extended Data Fig. 2, entry 5) or in other polar solvents (DMF or tetrahydrofuran (THF); Extended Data Fig. 2, entries 6 and 7). ^1H NMR spectroscopy confirms that **4c** (used as a model chlorination reagent) interacts with the DMSO solvent, activating the C–Cl bond (Supplementary Fig. 22)[69]. Hydroxyl radicals were detected by electron paramagnetic resonance spectroscopy during the $DMSO/O_2$-promoted dehydrochlorination process (Supplementary Fig. 23), indicating that dehydrochlorination involves a radical-mediated pathway. Radical trapping and radical clock experiments demonstrate the formation of carbon-centred radicals through the release of Cl˙ radicals (Supplementary Figs. 24 and 25). These results imply that $DMSO/O_2$ catalyses the dehydrochlorination step to afford HCl[16,70,71], with the formation of alkene (dominant) and alkanol (minor) intermediates (the hydroxyl oxygen may originate from O_2; Supplementary Fig. 26). The $NaNO_3$ promotes the oxidative decomposition of the dechlorinated (hydrocarbon component) polymer/solvent via C=C/C(OH)–C bond activation of the alkene and alkanol intermediates (Supplementary Figs. 27–29)[43–45,49].

In the final step, the PdO catalyses the chlorination of the arene substrate using HCl as the actual chlorination reagent[39,42,72].

Pd-catalysed C–H activation/chlorination was also investigated (Extended Data Fig. 3). Using HCl as the chlorination reagent, chlorination of **1a** does not proceed well without additional Cu catalyst and $NaNO_3$ (Extended Data Fig. 3, entries 1–4), which implies that the Cu catalyst and NO_3^- influence the activity of the Pd catalyst during the oxidative C–H chlorination reaction[40,73–75]. The model benzo[h]quinolinyl Pd(II) chloride intermediate was evaluated under the standard reaction conditions and affords chlorinated product **1b** only in the presence of both Cu and NO_3^- catalysts (Supplementary Fig. 30). X-ray photoelectron spectroscopy was used to confirm that the Cu and NO_3^- catalysts assist in the oxidation of the Pd catalyst in the presence of O_2 (Supplementary Fig. 31). These experiments imply that the Cu and NO_3^- catalysts act as redox mediators between O_2 and Pd(II) intermediates[73,75], promoting the formation of Pd(IV) intermediates, followed by reductive elimination to afford chlorinated products[39–41]. A series of tests to establish the nature of the active PdO catalyst was conducted, including hot filtration, elemental analysis, mercury poisoning, Pd(II) trapping and mass spectrometry, with all indicating that the active PdO catalyst is heterogeneous (Supplementary Figs. 32 and 33), although it cannot be excluded that, to a minor extent, the heterogeneous catalyst acts as a reservoir for homogeneous Pd species stabilized by the DMSO solvent[76]. Notably, without PdO, the combination of $Cu(NO_3)_2$ and $NaNO_3$ affords chlorinated product **1b** in 25% yield, presumably due to a less favourable Cu-catalysed chlorination pathway involving reduction elimination from a Cu(III) intermediate (Supplementary Fig. 34)[77,78].

Taken together, a tentative reaction sequence is shown in Fig. 4. Dechlorination catalysed by $DMSO/O_2$ (**a** to **b**) affords alkene and HCl intermediates (Supplementary Fig. 26). The hydrocarbon component undergoes oxidization to CO and H_2O via $NaNO_3$-promoted C–C bond cleavage (Supplementary Fig. 29), followed by oxidation of CO to CO_2 products (Pd-catalysed mainly). The HCl generated serves as the active chlorination reagent, which generates chlorinated arenes catalysed by the Pd species (**c** to **e**; Supplementary Fig. 35). Tentative reaction pathways for PVC- and PVDC-based chlorination reagents are provided in Supplementary Figs. 26, 29 and 34–36.

Life cycle assessment
To evaluate the environmental impact of the chlorination process, life cycle assessment (LCA) modelling was performed and compared with other chlorination strategies, with each system optimized to afford
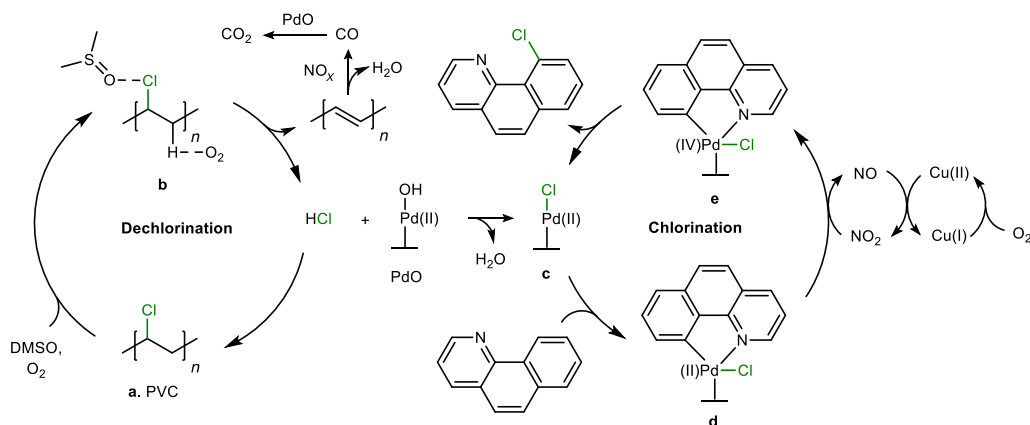
Fig. 4 | Mechanism study. Proposed reaction pathway based on PVC as the chlorination reagent.

1 kg of product. Note that the equivalent of PVC is considered to be incinerated for scenarios that do not employ PVC as the chlorination reagent and the production of valuable CO is not included. Details of LCA calculations are provided in Supplementary Figs. 37–40 and Supplementary Tables 5–7. LCA of the common chlorination route[39,41] using *N*-chlorosuccinimide as the chlorination reagent (scenario 1) for the generation of 2-(2-chloro-5-nitrophenyl)pyridine **12b**, an intermediate in the synthesis of the anticancer drug vismodegib, produces 9.18 kg of CO_2, whereas using PVC as the chlorination reagent (scenario 2), less than six times the amount of CO_2 is generated, that is, 1.41 kg, despite the latter route producing CO_2 gas as a by-product. The main contribution of the CO_2 generated from the *N*-chlorosuccinimide route consists of the production of the chlorination reagent itself and unrecoverable Pd(OAc)$_2$ catalyst required, whereas using PVC waste is free of charge and the heterogeneous PdO catalyst may be recovered (Supplementary Fig. 11). The PVC route was also compared with the recently published electrochemical chlorination strategy using PVC as a chlorination reagent for the generation of 1 kg of 1-(2-chlorophenyl)-pyrazole **19b** (compare scenarios 3 and 4)[34]. In the electrochemical process, a large excess of PVC and tetrabutylammonium tetrafluoroborate (NBu$_4$BF$_4$) containing electrolyte are needed (the expensive bis(2-ethylhexyl) phthalate additive was not included in the analysis). The LCA indicates that electrochemical chlorination will produce 54.62 kg of CO_2, which is over 20 times higher than the method reported here, which would produce 2.59 kg of CO_2. The main source of CO_2 is from the large quantity of NBu$_4$BF$_4$ electrolyte required. The LCA confirms that the method is more promising and less environmentally detrimental than other reported methods.

Conclusions

More sustainable alternatives to chlorinated compounds are a key goal in green chemistry, although in some cases, for example, in pharmaceutical products[79], it is unlikely that replacements will be identified in the near future. The choice of investing in greener chlorination approaches, or finding non-chlorinated alternatives, should be guided by a thorough assessment of the impact on both public health and the environment. Here we have shown that intractable chlorinated waste can be used as chlorination reagents to produce valuable aryl chloride products, with the hydrocarbon component being simultaneously mineralized. A new synthetic route to the FDA-approved drug, vismodegib, was developed, with the two Cl atoms in vismodegib derived from waste PVC water pipe. LCA indicates that this route has a lower environmental impact than the reported chlorination process[39,41]. Thus, this study charts a path for chlorinated wastes to be 'decommissioned' in a safe and sustainable way, simultaneously adding value to the process and additionally eliminating the need to manufacture unsustainable chlorination reagents. Note that chlorine production is the main

electricity-consuming process in the chemical industry[80] and is not sustainable unless the process is powered by renewable energy, hence using 'reclaimed' chlorine is advantageous. Future work will be focused on scaling up the reaction and extending the substrate scope, that is, to arenes without directing groups. Should it prove possible to chlorinate a broader range of arenes using this approach, then substantially larger quantities of chlorinated hydrocarbon waste could be valorized, helping to bridge the gap between chlorinated hydrocarbon waste and its application as chlorination reagents.

Online content

Any methods, additional references, Nature Portfolio reporting summaries, source data, extended data, supplementary information, acknowledgements, peer review information; details of author contributions and competing interests; and statements of data and code availability are available at https://doi.org/10.1038/s41557-024-01462-8.

References

1. Jiang, F. et al. N-terminal signal peptides facilitate the engineering of PVC complex as a potent protein delivery system. *Sci. Adv.* **8**, eabm2343 (2022).
2. Liu, D. et al. Standardized measurement of dielectric materials' intrinsic triboelectric charge density through the suppression of air breakdown. *Nat. Commun.* **13**, 6019 (2022).
3. Naclerio, N. D. et al. Controlling subterranean forces enables a fast, steerable, burrowing soft robot. *Sci. Robot.* **6**, eabe2922 (2021).
4. Kim, J., Zhang, G., Shi, M. & Suo, Z. Fracture, fatigue, and friction of polymers in which entanglements greatly outnumber cross-links. *Science* **374**, 212–216 (2021).
5. Frey, S. T. et al. Octopus-inspired adhesive skins for intelligent and rapidly switchable underwater adhesion. *Sci. Adv.* **8**, eabq1905 (2022).
6. Ferrer-Gago, F. J., Koh, L. Q. & Lane, D. P. Functionalized resins for the synthesis of peptide alcohols. *Chem. Eur. J.* **26**, 379–383 (2020).
7. Zhang, D. et al. Identification, occurrence, and cytotoxicity of haloanilines: a new class of aromatic nitrogenous disinfection byproducts in chloraminated and chlorinated drinking water. *Environ. Sci. Technol.* **56**, 4132–4141 (2022).
8. Jordan, A., Stoy, P. & Sneddon, H. F. Chlorinated solvents: their advantages, disadvantages, and alternatives in organic and medicinal chemistry. *Chem. Rev.* **121**, 1582–1622 (2021).
9. Jordan, A., Hall, C. G. J., Thorp, L. R. & Sneddon, H. F. Replacement of less-preferred dipolar aprotic and ethereal solvents in synthetic organic chemistry with more sustainable alternatives. *Chem. Rev.* **122**, 6749–6794 (2022).

10. Dutta, P. et al. A case study in green chemistry: the reduction of hazardous solvents in an industrial R&D environment. *Green Chem*. **24**, 3943–3956 (2022).

11. Hossain, A., Bhattacharyya, A. & Reiser, O. Copper's rapid ascent in visible-light photoredox catalysis. *Science* **364**, eaav9713 (2019).

12. Forbes, K. C. & Jacobsen, E. N. Enantioselective hydrogen-bond-donor catalysis to access diverse stereogenic-at-P(V) compounds. *Science* **376**, 1230–1236 (2022).

13. Bhutani, P. et al. U.S. FDA approved drugs from 2015–June 2020: a perspective. *J. Med. Chem*. **64**, 2339–2381 (2021).

14. Cao, H., Cheng, Q. & Studer, A. Radical and ionic meta-C–H functionalization of pyridines, quinolines, and isoquinolines. *Science* **378**, 779–785 (2022).

15. Fink, E. A. et al. Structure-based discovery of nonopioid analgesics acting through the α2A-adrenergic receptor. *Science* **377**, eabn7065 (2022).

16. Song, S. et al. DMSO-catalysed late-stage chlorination of (hetero) arenes. *Nat. Catal*. **3**, 107–115 (2020).

17. Liew, Z. & Guo, P. Human health effects of chemical mixtures. *Science* **375**, 720–721 (2022).

18. Atashgahi, S. et al. Prospects for harnessing biocide resistance for bioremediation and detoxification. *Science* **360**, 743–746 (2018).

19. Cowell, A. N. et al. Mapping the malaria parasite druggable genome by using in vitro evolution and chemogenomics. *Science*. **359**, 191–199 (2018).

20. Martín, A. J., Mondelli, C., Jaydev, S. D. & Pérez-Ramírez, J. Catalytic processing of plastic waste on the rise. *Chem* **7**, 1487–1533 (2021).

21. Zhang, M.-Q. et al. Catalytic strategies for upvaluing plastic wastes. *Chem* **8**, 2912–2923 (2022).

22. Ellis, L. D. et al. Chemical and biological catalysis for plastics recycling and upcycling. *Nat. Catal*. **4**, 539–556 (2021).

23. Jehanno, C. et al. Critical advances and future opportunities in upcycling commodity polymers. *Nature* **603**, 803–814 (2022).

24. Lee, K., Jing, Y., Wang, Y. & Yan, N. A unified view on catalytic conversion of biomass and waste plastics. *Nat. Rev. Chem*. **6**, 635–652 (2022).

25. Chu, M., Liu, Y., Lou, X., Zhang, Q. & Chen, J. Rational design of chemical catalysis for plastic recycling. *ACS Catal*. **12**, 4659–4679 (2022).

26. Lee, W.-T. et al. Mechanistic classification and benchmarking of polyolefin depolymerization over silica-alumina-based catalysts. *Nat. Commun*. **13**, 4850 (2022).

27. Zhang, F. et al. Polyethylene upcycling to long-chain alkylaromatics by tandem hydrogenolysis/aromatization. *Science* **370**, 437–441 (2020).

28. Conk, R. J. et al. Catalytic deconstruction of waste polyethylene with ethylene to form propylene. *Science* **377**, 1561–1566 (2022).

29. Hou, Q. et al. Upcycling and catalytic degradation of plastic wastes. *Cell Rep. Phys. Sci*. **2**, 100514 (2021).

30. Glas, D., Hulsbosch, J., Dubois, P., Binnemans, K. & De Vos, D. E. End-of-life treatment of poly(vinyl chloride) and chlorinated polyethylene by dehydrochlorination in ionic liquids. *ChemSusChem* **7**, 610–617 (2014).

31. Zhao, T. et al. A highly efficient approach for dehydrochlorinating polyvinyl chloride: catalysis by 1-butyl-3-methylimidazolium chloride. *Green Chem*. **12**, 1062–1065 (2010).

32. Chen, Y. et al. Catalytic dechlorination and charring reaction of polyvinyl chloride by CuAl layered double hydroxide. *Energy Fuels* **32**, 2407–2413 (2018).

33. Kots, P. A., Vance, B. C., Quinn, C. M., Wang, C. & Vlachos, D. G. A two-stage strategy for upcycling chlorine-contaminated plastic waste. *Nat. Sustain*. **6**, 1258–1267 (2023).

34. Fagnani, D. E., Kim, D., Camarero, S. I., Alfaro, J. F. & McNeil, A. J. Using waste poly(vinyl chloride) to synthesize chloroarenes by plasticizer-mediated electro(de)chlorination. *Nat. Chem*. **15**, 222–229 (2022).

35. Alberini, A. & Bartholomew, J. The determinants of hazardous waste disposal choice: an empirical analysis of halogenated solvent waste shipments. *Contemp. Econ. Policy* **17**, 309–320 (1999).

36. Pekelney, D. Hazardous waste generation, transportation, reclamation, and disposal: California's manifest system and the case of halogenated solvients. *J. Hazard. Mater*. **23**, 293–315 (1990).

37. Gan, G. et al. Nature of intrinsic defects in carbon materials for electrochemical dechlorination of 1,2-dichloroethane to ethylene. *ACS Catal*. **11**, 14284–14292 (2021).

38. Choi, C. et al. Efficient electrocatalytic valorization of chlorinated organic water pollutant to ethylene. *Nat. Nanotechnol*. **18**, 160–167 (2022).

39. Whitfield, S. R. & Sanford, M. S. Reactivity of Pd(II) complexes with electrophilic chlorinating reagents: isolation of Pd(IV) products and observation of C–Cl bond-forming reductive elimination. *J. Am. Chem. Soc*. **129**, 15142–15143 (2007).

40. Kakiuchi, F. et al. Palladium-catalyzed aromatic C–H halogenation with hydrogen halides by means of electrochemical oxidation. *J. Am. Chem. Soc*. **131**, 11310–11311 (2009).

41. Powers, D. C., Benitez, D., Tkatchouk, E., Goddard, W. A. III & Ritter, T. Bimetallic reductive elimination from dinuclear Pd(III) complexes. *J. Am. Chem. Soc*. **132**, 14092–14103 (2010).

42. Petrone, D. A., Ye, J. & Lautens, M. Modern transition-metal-catalyzed carbon–halogen bond formation. *Chem. Rev*. **116**, 8003–8104 (2016).

43. Liu, M. et al. Nitrogen dioxide catalyzed aerobic oxidative cleavage of C(OH)–C bonds of secondary alcohols to produce acids. *Angew. Chem. Int. Ed. Engl*. **58**, 17393–17398 (2019).

44. Liu, M. et al. Aerobic oxidative cleavage and esterification of C(OH)–C bonds. *Chem* **6**, 3288–3296 (2020).

45. Liu, M., Han, B. & Dyson, P. J. Simultaneous generation of methyl esters and CO in lignin transformation. *Angew. Chem. Int. Ed. Engl*. **61**, e202209093 (2022).

46. Liu, M. & Dyson, P. J. Direct conversion of lignin to functionalized diaryl ethers via oxidative cross-coupling. *Nat. Commun*. **14**, 2830 (2023).

47. McGivern, W. S., Derecskei-Kovacs, A., North, S. W. & Francisco, J. S. Computationally efficient methodology to calculate C–H and C–X (X=F, Cl, and Br) bond dissociation energies in haloalkanes. *J. Phys. Chem. A* **104**, 436–442 (2000).

48. Jaworski, J. S., Cembor, M. & Koliński, M. Electrostatic model of bond dissociation energies in polyhalogen methanes. *J. Phys. Org. Chem*. **19**, 276–280 (2006).

49. Liu, M., Yang, X. & Dyson, P. J. Chlorination of arenes via the degradation of toxic chlorophenols. *Proc. Natl Acad. Sci. USA*. **119**, e2122425119 (2022).

50. Wang, D., Weinstein, A. B., White, P. B. & Stahl, S. S. Ligand-promoted palladium-catalyzed aerobic oxidation reactions. *Chem. Rev*. **118**, 2636–2679 (2018).

51. Liu, F. et al. Transesterification catalyzed by ionic liquids on superhydrophobic mesoporous polymers: heterogeneous catalysts that are faster than homogeneous catalysts. *J. Am. Chem. Soc*. **134**, 16948–16950 (2012).

52. van Spronsen, M. A., Frenken, J. W. M. & Groot, I. M. N. Surface science under reaction conditions: CO oxidation on Pt and Pd model catalysts. *Chem. Soc. Rev*. **46**, 4347–4374 (2017).

53. Pearson, D. M., Conley, N. R. & Waymouth, R. M. Palladium-catalyzed carbonylation of diols to cyclic carbonates. *Adv. Synth. Catal*. **353**, 3007–3013 (2011).

54. Varga, M. et al. Adsorbed eutectic GaIn structures on a neoprene foam for stretchable MRI coils. *Adv. Mater.* **29**, 1703744 (2017).

55. Zhang, W., Zhang, T., Jiang, N. & Zhang, T. Chemical modification of neoprene rubber by grafting cardanol, a versatile renewable materials from cashew industry. *J. Polym. Res.* **27**, 163 (2020).

56. Genuino, H. C., Pilar Ruiz, M., Heeres, H. J. & Kersten, S. R. A. Pyrolysis of mixed plastic waste: predicting the product yields. *Waste Manag.* **156**, 208–215 (2023).

57. Yusuf, A. A. et al. Investigating the influence of plastic waste oils and acetone blends on diesel engine combustion, pollutants, morphological and size particles: dehalogenation and catalytic pyrolysis of plastic waste. *Energy Convers. Manag.* **291**, 117312 (2023).

58. Ceballos, D. M. et al. Perchloroethylene and dry cleaning: it's time to move the industry to safer alternatives. *Front. Public Health* **9**, 638082 (2021).

59. Davenport, E., Negru, D. E., Badman, G., Lindsay, D. M. & Kerr, W. J. Robust and general late-stage methylation of aryl chlorides: application to isotopic labeling of drug-like scaffolds. *ACS Catal.* **13**, 11541–11547 (2023).

60. Alder, C. M. et al. Updating and further expanding GSK's solvent sustainability guide. *Green Chem.* **18**, 3879–3890 (2016).

61. Vyas, P. V., Bhatt, A. K., Ramachandraiah, G. & Bedekar, A. V. Environmentally benign chlorination and bromination of aromatic amines, hydrocarbons and naphthols. *Tetrahedron Lett.* **44**, 4085–4088 (2003).

62. Firouzabadi, H., Iranpoor, N. & Shiri, M. Direct and regioselective iodination and bromination of benzene, naphthalene and other activated aromatic compounds using iodine and bromine or their sodium salts in the presence of the $Fe(NO_3)_3 \cdot 1.5N_2O_4$/charcoal system. *Tetrahedron Lett.* **44**, 8781–8785 (2003).

63. Kalyani, D., Dick, A. R., Anani, W. Q. & Sanford, M. S. A simple catalytic method for the regioselective halogenation of arenes. *Org. Lett.* **8**, 2523–2526 (2006).

64. Misal, B., Palav, A., Ganwir, P. & Chaturbhuj, G. Activator free, expeditious and eco-friendly chlorination of activated arenes by *N*-chloro-*N*-(phenylsulfonyl)benzene sulfonamide (NCBSI). *Tetrahedron Lett.* **63**, 152689 (2021).

65. Sekulic, A. et al. Efficacy and safety of vismodegib in advanced basal-cell carcinoma. *N. Engl. J. Med.* **366**, 2171–2179 (2012).

66. Yu, Q., Hu, L. A., Wang, Y., Zheng, S. & Huang, J. Directed meta-selective bromination of arenes with ruthenium catalysts. *Angew. Chem. Int. Ed. Engl.* **54**, 15284–15288 (2015).

67. Umei, K. et al. Identification of novel 1,2,3,6-tetra hydropyridyl-substituted benzo[*d*]thiazoles: lead generation and optimization toward potent and orally active EP_1 receptor antagonists. *Bioorg. Med. Chem.* **25**, 3406–3430 (2017).

68. Dhanya, R.-P. et al. Design and synthesis of an orally active metabotropic glutamate receptor subtype-2 (mGluR2) positive allosteric modulator (PAM) that decreases cocaine self-administration in rats. *J. Med. Chem.* **54**, 342–353 (2011).

69. Eytel, L. M., Fargher, H. A., Haley, M. M. & Johnson, D. W. The road to aryl CH···anion binding was paved with good intentions: fundamental studies, host design, and historical perspectives in CH hydrogen bonding. *Chem. Commun.* **55**, 5195–5206 (2019).

70. Wang, L., Zhang, R.-Z., Deng, R. & Luo, Y.-H. Oxygen-induced enhancement in low-temperature dechlorination of PVC: an experimental and DFT study on the oxidative pyrolysis process. *ACS Sustain. Chem. Eng.* **9**, 2835–2843 (2021).

71. Zhang, R.-Z., Wang, L.-Z., Deng, R.-Q. & Luo, Y.-H. Inhibition on chloroaromatics during thermal conversion processes of municipal solid waste by oxygen-induced low-temperature pre-dechlorination and hydrogen-assisted in-situ Cl capture. *Fuel Process. Technol.* **237**, 107445 (2022).

72. Song, B., Zheng, X., Mo, J. & Xu, B. Palladium-catalyzed monoselective halogenation of C–H bonds: efficient access to halogenated arylpyrimidines using calcium halides. *Adv. Synth. Catal.* **352**, 329–335 (2010).

73. Piera, J. & Bäckvall, J.-E. Catalytic oxidation of organic substrates by molecular oxygen and hydrogen peroxide by multistep electron transfer—a biomimetic approach. *Angew. Chem. Int. Ed. Engl.* **47**, 3506–3523 (2008).

74. Pye, D. R. & Mankad, N. P. Bimetallic catalysis for C–C and C–X coupling reactions. *Chem. Sci.* **8**, 1705–1718 (2017).

75. Kim, U. B., Jung, D. J., Jeon, H. J., Rathwell, K. & Lee, S.-G. Synergistic dual transition metal catalysis. *Chem. Rev.* **120**, 13382–13433 (2020).

76. Dyson, P. J. & Jessop, P. G. Solvent effects in catalysis: rational improvements of catalysts via manipulation of solvent interactions. *Catal. Sci. Technol.* **6**, 3302–3316 (2016).

77. Chen, X., Hao, X.-S., Goodhue, C. E. & Yu, J.-Q. Cu(II)-catalyzed functionalizations of aryl C–H bonds using O_2 as an oxidant. *J. Am. Chem. Soc.* **128**, 6790–6791 (2006).

78. Yang, L., Lu, Z. & Stahl, S. S. Regioselective copper-catalyzed chlorination and bromination of arenes with O_2 as the oxidant. *Chem. Commun.* **14**, 6460–6462 (2009).

79. Chiodi, D. & Ishihara, Y. 'Magic chloro': profound effects of the chlorine atom in drug discovery. *J. Med. Chem.* **66**, 5305–5331 (2023).

80. Worrell, E., Phylipsen, D., Einstein, D. & Martin, N. *Energy Use and Energy Intensity of the U.S. Chemical Industry* Technical Report LBNL-44314 (US EPA, 2000).

Methods

General procedures

7,8-Benzoquinoline **1a** (0.25 mmol), PVC water pipe (1.5 equiv., 0.375 mmol), $Cu(NO_3)_2 \cdot 3H_2O$ (20%, 0.05 mmol), PdO (5%, 0.0125 mmol), $NaNO_3$ (20%, 0.05 mmol), biphenyl (0.2 mmol, internal standard) and DMSO (2 ml) were added into a glass insert vial of the autoclave and charged with O_2 (3 bar). The reactor was heated to 140 °C for 15 h. After cooling to room temperature, the gas products were collected with a Tedlar gas-sampling bag (Sigma-Aldrich) for analysis by GC. Ethyl acetate (3 × 3 ml) and an aqueous saturated brine solution (5 ml) was added to the reaction mixture to extract the organic products. The combined organic phase was used for analysis. Further purification was achieved using silica gel chromatography (hexane/ethyl acetate as eluent if not specified) when required.

Analytical methods

Qualitative and quantitative analysis of gas-phase products was performed by GC using an Agilent 7890B instrument equipped with a hydrogen flame-ionization detector and a thermal conductivity detector. The GC yield was determined based on standard gas mixtures and integrated peak areas. Qualitative and quantitative analysis of crude liquid products was performed using an Agilent 7000C GCMS equipped with a hydrogen flame-ionization detector, electron ionization mass detector and HP-5 non-polar column. The GC yield was determined on the basis of internal standard curves and integrated peak areas.

Determination of the molecular weight and polydispersity of the polymers was performed using GPC on an Agilent 390-MDS equipped with a refractive index detector, and dual-angle light scattering detector. THF was used as eluent. For the measurement after reaction, brine (10 ml) was added to the DMSO solution (2 ml) and the organic components were extracted with THF (3 × 5 ml). The THF extract was used for GPC.

^{1}H and ^{13}C NMR spectra were recorded on a Bruker Avance III HD 400 instrument equipped with a 5 mm BBFO probe. DMSO-d_6 or $CDCl_3$ were used as solvent. DMSO-d_6 was used as the reaction solvent for the reaction that was monitored by ^{1}H NMR spectroscopy. After centrifuging to remove the PdO catalyst, the crude reaction mixture (0.2 ml) was diluted with DMSO-d_6 or THF-d_8 (0.4 ml) and directly used for the ^{1}H NMR experiment.

Other methods are included in the Supplementary Information.

Author contributions

M.L. and P.J.D. designed the research, analysed data and wrote the paper. M.L. and X.W. performed the research.

Competing interests

The catalytic method is described in a patent invented by M.L. and P.J.D. (EP patent, No. 23170105.3). The other authors declare no competing interests.

Additional information

Extended data is available for this paper at https://doi.org/10.1038/s41557-024-01462-8.

Supplementary information The online version contains supplementary material available at https://doi.org/10.1038/s41557-024-01462-8.

Correspondence and requests for materials should be addressed to Paul J. Dyson.

Peer review information *Nature Chemistry* thanks Haohong Duan, Andrew Jordan, Bert Weckhuysen and the other, anonymous, reviewer(s) for their contribution to the peer review of this work.

Reprints and permissions information is available at www.nature.com/reprints.
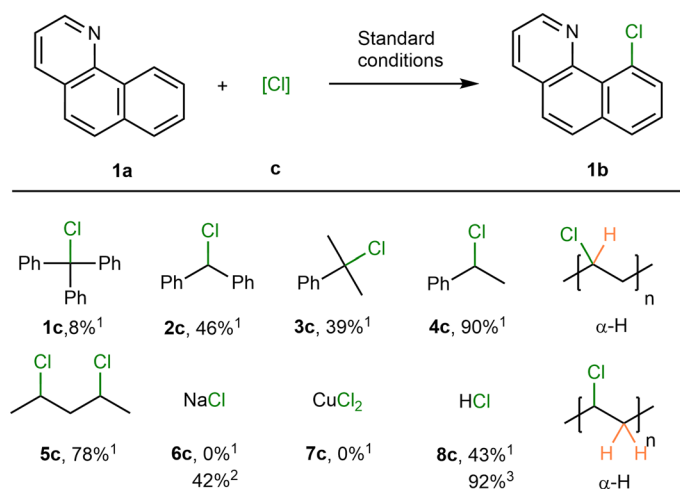
Extended Data Fig. 1 | Application of model organic and inorganic chlorides as chlorination reagents. Standard conditions: (1) 7,8-benzoquinoline **1a** (0.25 mmol), chlorides (1.5 equiv., 0.375 mmol), Cu(NO$_3$)$_2$·3H$_2$O (20 mol%, 0.05 mmol), PdO (5 mol%, 0.0125 mmol), NaNO$_3$ (20 mol%, 0.05 mmol), biphenyl (0.2 mmol, internal standard), DMSO (2 mL), O$_2$ (3 bar), 140 °C, 15 h. (2) with acetic acid (3 equiv., 0.75 mmol). (3) with HCl (3 equiv., 0.75 mmol).
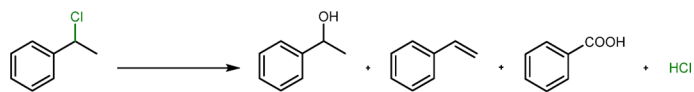
Entry	Catalyst	Gas	Solvent	Phenylethanol (%)	Styrene (%)	Benzoic acid (%)
1	CuO	O_2	DMSO	2	0	70
2	$NaNO_3$	O_2	DMSO	0	0	81
3	PdO	O_2	DMSO	15	82	3
4		O_2	DMSO	17	80	3
5		N_2	DMSO	12	9	0
6		O_2	DMF	0	0	0
7		O_2	THF	0	0	0

Extended Data Fig. 2 | Evaluation of dechlorination and C=C/C(OH)−C bond activation using model compound 4c. Reaction conditions: substrate **4c** (0.25 mmol), catalyst (20 mol%, 0.05 mmol), solvent (2 mL), biphenyl (0.2 mmol), gas (1 bar), 140 °C, 3 h.
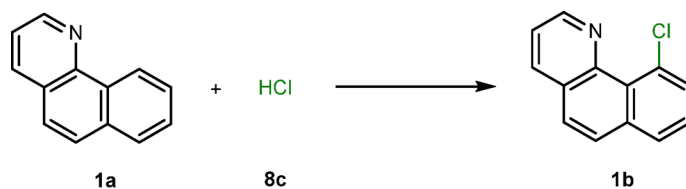
Entry	[Pd]	[Cu]	NaNO$_3$	Yield of **1b** (%)
1	PdO	Cu(NO$_3$)$_2$	NaNO$_3$	92
2	PdO	CuCl$_2$		5
3	PdO		NaNO$_3$	0
4	PdO			0
5		Cu(NO$_3$)$_2$	NaNO$_3$	25

Extended Data Fig. 3 | Optimization of the chlorination reaction using HCl as a chlorination reagent. Standard conditions: 7,8-benzoquinoline **1a** (0.25 mmol), HCl (3 equiv., 0.75 mmol), Cu(NO$_3$)$_2$·3H$_2$O (20 mol%, 0.05 mmol), PdO (5 mol%, 0.0125 mmol), NaNO$_3$ (20 mol%, 0.05 mmol), biphenyl (0.2 mmol, internal standard), DMSO (2 mL), O$_2$ (3 bar), 140 °C, 15 h.